ELSEVIER

Solid State Nuclear Magnetic Resonance 13 (1998) 175–182

SOLID STATE
Nuclear Magnetic
Resonance

Characterization of silicon sites in monoclinic zeolite ZSM-5 using ^{29}Si magic angle spinning (MAS) nuclear magnetic resonance (NMR) and molecular modelling

C. Sivadinarayana, V.R. Choudhary, R. Vetrivel, S. Ganapathy *

National Chemical Laboratory, Pune 411 008, India

Received 1 July 1998; accepted 10 August 1998

Abstract

An attempt has been made to correlate the experimentally observed ^{29}Si MAS NMR chemical shifts of monoclinic phase of highly siliceous ZSM-5 with their electronic properties. In order to incorporate the influence of next neighbor atoms on the ^{29}Si chemical shielding of central SiO_4, a pentameric cluster model ($H_{12}Si_5O_{16}$) has been chosen. Each of the 24 crystallographically distinct Si sites, of ZSM-5 framework has been modelled by such cluster models. Based on semi-empirical quantum chemical calculations, a multiple linear regression analysis of the various electronic properties with the ^{29}Si chemical shifts has been attempted. The relative difference in ^{29}Si chemical shifts for the Si sites in ZSM-5 is reasonably accounted, although quantitative prediction may require non-empirical quantum chemical calculations.

Keywords: ZSM-5; Quantum calculation; Molecular modelling; MAS NMR

1. Introduction

The structure determination of microsporous zeolites is mainly carried out from powder data using Rietveld analysis. Single crystal diffraction data on zeolites are often limited due to difficulties in the synthesis of large diffraction quality single crystals. There are several attempts to develop experimental and computational methodologies, which are useful to assist solving the zeolite structure. One such attempt is to understand the relationship between the geometry of the Si sites and the ^{29}Si MAS NMR chemical shift [1]. Thus, it should be possible to derive structural features of crystallographically distinct Si sites in the zeolite from ^{29}Si MAS NMR spectra.

There have been many empirical, semi-empirical and non-empirical calculation approaches to locate the preferential isomorphous substitution of several elements in place of zeolite framework. Fripiat et al. [2] and Derouane and Fripiat [3] used ab initio calculations on dimer clusters of ZSM-5 and ZSM-11 to propose preferential substitution sites for aluminum in different zeolites. O'Malley and Dwyer [4] performed ab initio calculations to reveal the substi-

* Corresponding author. E-mail: ganpat@ems.ncl.res.in

0926-2040/98/$17.00
PII: S0926-2040(98)00079-4

tution of aluminum in the Theta-1 framework. The semi-empirical quantum chemical calculations using MNDO Hamiltonian has been adopted to calculate the substitution energy of boron for Si at different probable framework sites in the ZSM-5 structure [5]. EHMO calculations on ferrisilicate zeolite models were used to find out the preferential substitution sites for iron in ZSM-5 framework [6]. These studies have established the relationship between the substitution energy and the local geometry of T-site. Further, it was also shown that the net charge on bridging oxygen atoms has linear relation with the local geometry as well as the catalytic activity in acid-catalyzed reactions [7]. Recently, Alvarado Swaisgood et al. [8] have used ab initio calculations for studying the electronic properties of 12 different Si sites of ZSM-5 framework. They also proposed a model to explain the dependence of the electronic property of the cluster models on the geometry of Si sites. Schroder et al. [9] used lattice defect energy minimization method to locate the preferential sites of aluminum substitution for silicon in the monoclinic phase of the ZSM-5 framework. Thus, there are several successful examples in the literature where the local structure of Si sites in zeolites is correlated to their electronic properties.

Fyfe et al. [1] have established a linear correlation between ^{29}Si MAS NMR chemical shift and Si–Si distance. Such an empirical correlation is found to be useful in resolving the space group ambiguity in new zeolite structures [10,11]. Further, they are useful in making unique Si site assignments using 2-D MAS NMR spectroscopy. There are also studies [12–18] which bring out the linear correlation between ^{29}Si MAS NMR chemical shift and Si–O–Si bond angles in various zeolites. However, to the best of our knowledge, there has been no attempt to systematically correlate the ^{29}Si MAS NMR chemical shifts to electronic properties, which can be calculated by quantum chemical methods.

In this paper, we use the AM1 method [19] to study the electronic properties of pentameric cluster models pertaining to all the 24 crystallographically distinct Si sites in the monoclinic phase of silicious ZSM-5 (silicalite-I). The monoclinic phase of ZSM-5 is chosen as the test case to study these correlations, since accurate X-ray diffraction [20] and ^{29}Si MAS NMR [1,21,22] data have been reported.

2. Methodology

2.1. Experimental

For recording ^{29}Si MAS NMR spectrum, high silica ZSM-5 (silicalite-1) was prepared by hydrothermal synthesis from a gel composition; tetrapropyl ammonium bromide: SiO_2:H_2O = 1:70:107 at 443 K for a period of 8 days. The synthesized material was calcined at 723 K in static air for 10 h. The synthesis conditions to get a defect free and highly crystalline material were optimized as described elsewhere [21]. The calcined material was fully characterised and found to conform to the monoclinic phase of silicalite-1 [20]. ^{29}Si MAS NMR spectra was recorded at the Larmor frequency of 59.621 MHz using Bruker MSL-300 FT-NMR spectrometer. The various experimental conditions, such as magnet shimming, magic angle setting, etc., were optimised so that the various crystallographically distinct Si sites could be resolved to the maximum extent possible in the ^{29}Si MAS spectra.

2.2. Molecular modelling

The semi-empirical quantum chemical cluster calculations were carried out using AM1 Hamiltonian [19], using the AMPAC code (QCPE Programme No. 506). The applicability of the AM1 technique and the several calculation features are reported by Stewart [23]. Although the absolute values of energy calculated using AM1 Hamiltonian do not carry much chemical meaning, they can however be used to compare the results of calculations from similar cluster models. We have used this approach to perform calculations on cluster models representing the 24 crystallographically distinct Si sites in silicalite-1. A pentameric cluster model with the molecular formula $Si\{OSi(OH)_3\}_4$ was generated for each of the 24 Si sites in silicalite-1. This cluster model represents the central SiO_4 unit in a crystallographic site linked tetrahedrally to four more SiO_4 units by corner sharing of the oxygen atoms. The valency of boundary oxygen atoms is saturated by hydrogen atoms. These hydrogen atoms lie along the vector of the adjacent 'Si' sites in the framework and the O–H bond distance is 0.97 A°. The secondary building unit containing 24 unique Si sites, which form the asym-

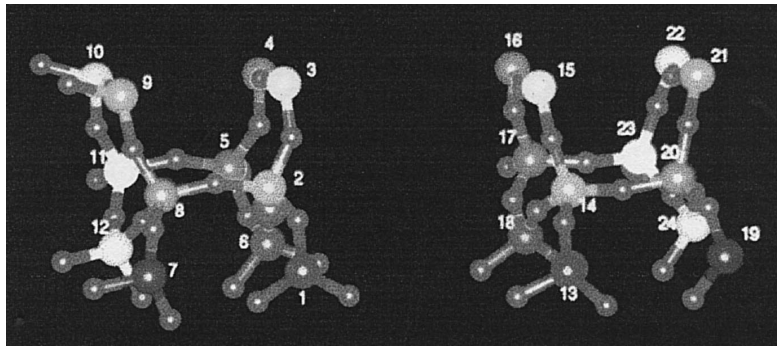

Fig. 1. The secondary building unit in the monoclinic phase of ZSM-5. The 24 crystallographically distinct Si sites are numbered as per the X-ray structure [20].

metric unit for the monoclinic phase of the silicalite-1, is shown in Fig. 1. The cluster models used in the present study were derived from the crystal structure reports of van Koningsveld et al. [20]. The calculations were performed on a *SiliconGraphics Indigo*^{2} workstation using molecular modelling software developed and distributed by Biosym Technologies, USA.

3. Results and discussion

3.1. ^{29}Si *MAS NMR chemical shifts*

A typical ^{29}Si MAS NMR spectrum obtained for silicalite-1 is shown in Fig. 2. Except for the overlap of few peaks, which are not resolved, the entire spectral manifold can be assigned to 24 crystallographically distinct Si sites as shown. The experimentally observed ^{29}Si MAS chemical shifts (δ ppm, from TMS) are given in Table 1, together with Si resonance assignments and the three dimensional connectivity as verified by 2-D NMR measurements [1,22].

3.2. *AM1 calculations on 24 cluster models*

In Table 1, the local geometry of the 24 Si sites is also included. Each of the Si sites is coordinated to four oxygen atoms. The average of four Si–O bond distances $\langle$Si–O$\rangle$ and the four Si–O–Si bond angles $\langle$Si–O–Si$\rangle$ for each Si site are listed in Table 1. The neighboring silicon atoms to the central silicon, which are bridged through oxygen atoms are also given in Table 1. The molecular graphics picture of the typical pentamer cluster model is shown in Fig. 3. As mentioned earlier, 24 such cluster models, derived from the secondary building unit shown in Fig. 1, have been generated to represent all the crystallographically distinct Si sites. The electronic properties calculated for all such clusters are given in Table 2.

The AM1 total energy values calculated for the 24 cluster models are given in Table 2. These values are dependent on the geometry of cluster models, as expected. However, there was poor correlation between the total energy values and the ^{29}Si MAS

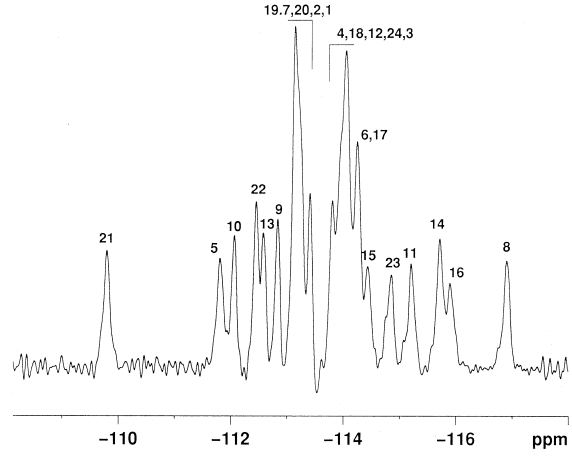

Fig. 2. Resolution enhanced ^{29}Si MAS spectrum of high silica zeolite silicalite-1 exhibiting the crystallographically distinct Si sites in the monoclinic ZSM-5 framework. Here decreasing values of δ denote increasing shielding from Si_{21} to Si_8. Assignments of the ^{29}Si peaks determined by 2-D NMR are also shown.

Table 1
The local geometry and the neighboring Si sites for each of the 24 Si sites in the monoclinic phase of silicalite-1

Central silicon	⟨Si–O⟩ bond distance (Å)	⟨Si–O–Si⟩ bond angle (degrees)	Neighboring silicon atoms to the central silicon[a]	^{29}Si chemical shift (ppm)[b]
Si_1	1.592	153.447	Si_2,Si_{16},Si_{17},Si_{22}	–
Si_2	1.580	153.155	Si_1,Si_3,Si_6,Si_8	–
Si_3	1.600	153.000	Si_2,Si_4,Si_{18},Si_{24}	−114.24
Si_4	1.600	151.090	Si_3,Si_5,Si_{13},Si_{19}	–
Si_5	1.595	149.498	Si_4,Si_6,Si_{11},Si_{13}	−111.69
Si_6	1.598	155.410	Si_2,Si_5,Si_{15},Si_{21}	–
Si_7	1.595	152.050	Si_8,Si_{16},Si_{19},Si_{23}	−113.22
Si_8	1.587	158.878	Si_2,Si_7,Si_9,Si_{12}	−116.94
Si_9	1.600	150.790	Si_8,Si_{10},Si_{18},Si_{21}	−112.79
Si_{10}	1.595	150.350	Si_9,Si_{11},Si_{13},Si_{22}	−112.00
Si_{11}	1.593	154.763	Si_5,Si_{10},Si_{12},Si_{19}	−115.07
Si_{12}	1.595	153.900	Si_8,Si_{11},Si_{15},Si_{24}	–
Si_{13}	1.548	151.282	Si_4,Si_5,Si_{10},Si_{14}	−112.66
Si_{14}	1.595	155.580	$Si_{13}Si_{15}$,Si_{18},Si_{20}	−115.88
Si_{15}	1.598	154.330	Si_6,Si_{12},Si_{14},Si_{16}	−114.52
Si_{16}	1.592	156.920	Si_1,Si_7,Si_{15},Si_{17}	−116.01
Si_{17}	1.590	153.215	Si_1,Si_{16},Si_{18},Si_{23}	−114.40
Si_{18}	1.600	152.150	Si_3,Si_9,Si_{14},Si_{17}	–
Si_{19}	1.597	151.570	Si_4,Si_7,Si_{11},Si_{20}	−113.22
Si_{20}	1.575	152.995	Si_{14},Si_{19},Si_{21},Si_{24}	−113.22
Si_{21}	1.630	147.110	Si_6,Si_9,Si_{20},Si_{22}	−109.80
Si_{22}	1.600	151.040	Si_1,Si_{10},Si_{21},Si_{23}	−112.51
Si_{23}	1.592	155.010	Si_7,Si_{17},Si_{22},Si_{24}	−114.73
Si_{24}	1.593	152.990	Si_3,Si_{12},Si_{20},Si_{23}	–

[a] Ref. [20].
[b] From the ^{29}Si MAS spectrum (ppm from TMS).

NMR chemical shift. The present calculations take into consideration the atoms in three coordinations around Si. By this cluster model (Fig. 3), the influence of geometric factors such as Si–O, O–Si–O, Si–O–Si and Si–O–Si–O are taken care of. However, the influence of the geometry factor—Si–O–Si–O could not be studied by the present cluster model. Thus a large cluster model and more elaborate quantum chemical calculations may lead to better correlations. But the calculations become computationally demanding. Although the total energy value is a function of the geometry of the whole cluster, the ^{29}Si chemical shifts are more influenced by the atoms immediately surrounding the Si site and less influenced by the atoms on the boundary of the cluster. Hence, the net charges on various atoms of the present cluster model (Fig. 3) were analysed (Table 2). A distinct variation in the net atomic charges between atoms at the core and periphery of the clusters was observed. The net atomic charge on the central Si is found to vary between 2.021 and 2.051, and hence its correlation with the chemical shift was first attempted. However, the correlation coefficient is found to be poor ($R = 0.40$, Table 3). Similarly, a correlation of the observed chemical shifts with the net atomic charge on the peripheral silicon, which varies in the range 1.987–2.020, was next attempted. The correlation coefficient ($R = 0.58$) is found to be similar. The dependence of the ^{29}Si chemical shift on any other single electronic property, such as the average net charge on oxygen atoms of the central SiO_4 unit $\langle q_o \rangle$ and the energy difference between the highest occupied molecular orbital (HOMO) and the lowest unoccupied molecular orbital (LUMO) (i.e., the band gap ΔE), also do not show good correlation. The results of these

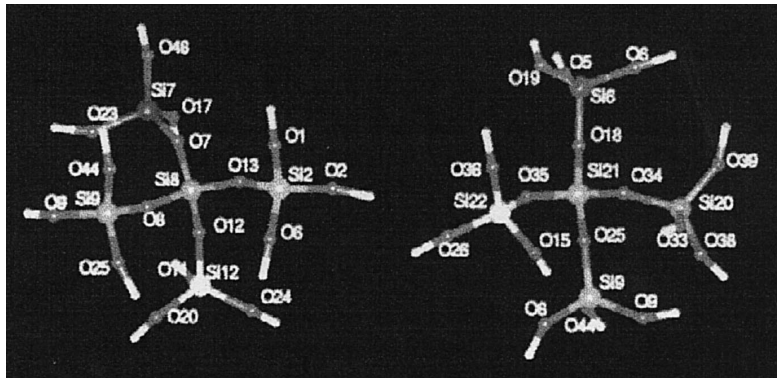

Fig. 3. Pentameric cluster models centered at Si_8 and Si_{21} sites corresponding to the ^{29}Si resonance at the high and low field extremes of ^{29}Si MAS NMR spectrum.

analyses are included in Table 3 in the form of correlation coefficients. This suggests that mutually independent electronic properties are likely to influence the chemical shift in a collective manner. When a multiple correlation analysis using various electronic properties (q_{Si}, $q_{p\text{-}Si,}$ q_0, total energy, band

Table 2
The electronic properties of the pentamer cluster models representing the 24 Si sites in the monoclinic phase of silicalite-1

Central silicon	Net charge on central silicon (q_{si})	Average net charges on four neighboring Si sites $\langle q_{si} \rangle$	Average net charges on four oxygen atoms coordinated to central Si $\langle q_o \rangle$	Total energy (ev)
Si_1	2.0344	2.0076	−0.9687	−5726.610
Si_2	2.0500	2.0144	−0.9677	−5726.220
Si_3	2.0309	2.0108	−0.9732	−5726.550
Si_4	2.0269	2.0050	−0.9891	−5726.901
Si_5	2.0375	2.0015	−0.9578	−5726.390
Si_6	2.0206	2.0008	−0.9727	−5727.053
Si_7	2.0417	2.0199	−0.9636	−5726.192
Si_8	2.0228	2.0099	−0.9902	−5726.778
Si_9	2.0497	2.0050	−0.9665	−5726.040
Si_{10}	2.0348	2.0101	−0.9741	−5726.364
Si_{11}	2.0229	2.0063	−0.9833	−5726.026
Si_{12}	2.0508	2.0184	−0.9648	−5725.142
Si_{13}	2.0315	2.0042	−0.9668	−5726.883
Si_{14}	2.0258	2.0097	−0.9766	−5726.900
Si_{15}	2.0364	2.0178	−0.9686	−5726.429
Si_{16}	2.0364	2.0178	−0.9686	−5726.429
Si_{17}	2.0344	2.0190	−0.9641	−5726.490
Si_{18}	2.0410	2.0126	−0.9688	−5726.602
Si_{19}	2.0229	2.0100	−0.9651	−5726.727
Si_{20}	2.0369	2.008	−0.9844	−5726.724
Si_{21}	2.0415	1.9868	−0.9610	−5726.910
Si_{22}	2.0354	1.9868	−0.9742	−5726.910
Si_{23}	2.0301	2.0125	−0.9823	−5726.679
Si_{24}	2.0268	2.0133	−0.9718	−5726.492

Table 3
Correlation between the experimental chemical shifts and the electronic or geometric properties[a]

Electronic or geometric property					Correlation coefficient (R)
X_1	X_2	X_3	X_4	X_5	
q_{si}					0.40
$\langle q_o \rangle$					0.52
$\langle q_{si} \rangle$					0.58
q_{Si}	$\langle q_0 \rangle$	$\langle q_{p\text{-}Si} \rangle$	total energy	band gap	0.82
⟨Si–O⟩					0.11
⟨Si–O–Si⟩					0.98

[a]Using equation: $Y = C_0 + C_1X_1 + C_2X_2 + C_3X_3 + C_4X_4 + C_5X_5$.

gap) is performed, there is a significant improvement in the correlation coefficient ($R = 0.82$) (Table 3).

We have carried out a detailed analysis of the space filling contours for the frontier molecular orbitals of all the 24 crystallographically distinct Si sites. In this perspective, we rationalise the observed chemical shielding for the extreme resonances, namely, Si_{21} and Si_8, for which the experimentally determined chemical shift dispersion is the largest. They typically represent resonances, which are at the shielding and deshielding extremes of the spectrum corresponding to -116.94 to -109.80 ppm, respectively. The band gap, ΔE, enters the expression for the paramagnetic part of the principal components of the chemical shielding tensor [24]. Considering HOMO and LUMO, we calculate ΔE to be 9.20 and 9.66 eV for Si_{21} and Si_8, respectively (Table 4). Since δ_p is inversely related to ΔE, the small value of ΔE for Si_{21} implies a large paramagnetic contribution and hence high deshielding. Similarly, for Si_8 the large value of ΔE implies high shielding, thus displacing Si_{21} and Si_8 to the two extremes of the ^{29}Si MAS spectrum. It is conceivable that with better quantum chemical methods it would be possible to calculate the frontier orbital characteristics more accurately. However, as mentioned earlier, the chemical shifts of all the peaks can be rationalised on a finer scale only by a consideration of all the electronic properties.

The frontier molecular orbital characteristics also provide a means of visualising the overall symmetry of the electronic shielding. The condensed nature of HOMO and the diffusive nature of LUMO in the cluster can be derived from the respective atomic orbitals contributing to it. The HOMO is mostly formed by the 2p orbitals of oxygen, while the LUMO is formed by the 3s orbitals of the peripheral silicons. Further, the electron density contours show little departure from spherical symmetry, thus depicting the overall T_d symmetry of the pentameric clusters, rather than the symmetry of the orbitals. For the Si in tetrahedral symmetry, the anisotropy of chemical shielding is however very small due to a slight disruption in the local T_d symmetry. This is supported by the absence of spinning side bands in the ^{29}Si MAS experiments. The chemical shielding tensor, therefore, is nearly isotropic.

We find that a correlation based on multiple regression analysis using the electronic properties ($R = 0.82$) is considerably lower than a linear regression analysis with a single geometric parameter, namely ⟨Si–O–Si⟩ angle ($R = 0.98$). Fig. 4 shows a

Table 4
The Eigen values of the frontier molecular orbitals in the pentameric cluster models used to represent the 24 Si sites in ZSM-5

Site number	Electron density maximum values (e/a.u.^{3})	HOMO (eV)	LUMO (eV)	Band gap (eV)
1	2207.86	−11.16	1.81	−9.35
2	2059.47	−11.21	1.91	−9.30
3	2216.22	−11.22	1.77	−9.45
4	1871.56	−11.44	1.70	−9.74
5	2116.19	−11.14	2.00	−9.14
6	2227.62	−11.32	1.79	−9.51
7	2252.47	−11.05	1.99	−9.06
8	2080.95	−11.44	1.78	−9.66
9	2330.75	−11.19	1.69	−9.50
10	2160.91	−11.08	1.58	−9.50
11	2222.85	−11.26	1.83	−9.43
12	2109.80	−10.40	1.71	−8.69
13	2174.51	−11.22	1.90	−9.31
14	2244.06	−11.24	1.74	−9.50
15	2328.75	−11.14	1.89	−9.25
16	2007.2	−11.14	1.89	−9.13
17	2307.30	−11.06	1.93	−9.37
18	2334.05	−11.27	1.90	−9.07
19	2123.81	−11.07	2.01	−9.62
20	2198.25	−11.35	1.73	−9.23
21	2163.67	−11.21	1.91	−9.20
22	2186.94	−11.01	1.81	−9.35
23	2265.45	−11.20	1.86	−9.35
24	2149.36	−11.02	1.90	−9.21

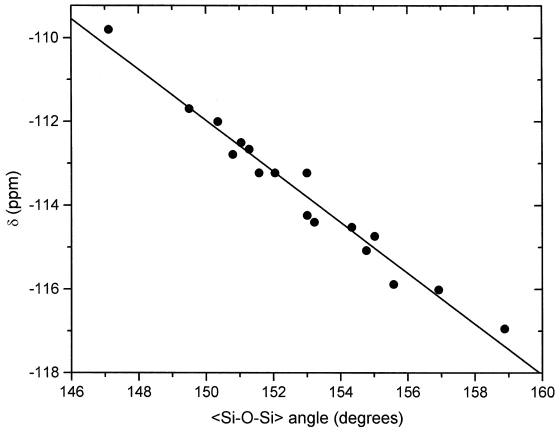

Fig. 4. Plot of ⟨Si–O–Si⟩ bond angle vs. ^{29}Si chemical shift showing a linear correlation.

plot of ⟨Si–O–Si⟩ bond angle vs. the ^{29}Si MAS chemical shift for the various Si sites. A crucial point in this analysis is that subtle changes in the geometry of T-site, such as those on the T–O–T angle, are accurately measured by X-ray diffraction methods, and they, in turn, translate into geometry dependent electronic properties that vary from site to site. It is, therefore, not surprising that an experimentally measured parameter such as T–O–T angle correlates remarkably well with the experimental chemical shifts. Although the electronic properties explain the qualitative variations in ^{29}Si chemical shifts for various sites, more accurate quantum chemical calculations, such as ab initio and density functional approaches, are needed to further improve the numerical accuracy of the calculations involving electronic properties. Further, considerations of long range interactions and geometry optimisation are required so that chemical shifts can be more accurately predicted using electronic properties.

4. Conclusions

We have shown that the experimentally observed ^{29}Si chemical shifts of monoclinic ZSM-5 correlate ($R = 0.82$) well with the electronic properties (charge on central Si, charge on peripheral Si and O, total energy and band gap) when quantum chemical calculations were performed using AM1 model and a pentameric cluster for the central silicon. From the analysis of the frontier molecular orbital contours for the clusters centred at Si_{21} and Si_8, the dependence of the chemical shift on the paramagnetic contributions is clearly brought out. It is finally suggested that this electronic property chemical shift correlation can be extended to other high silica zeolites using similar cluster models.

Acknowledgements

CS gratefully acknowledges Council of Scientific and Industrial Research (CSIR), New Delhi, for the financial assistance in the form of a research fellowship. The authors thank Professor S. Subramanian for discussions.

References

[1] C.A. Fyfe, H. Grondey, Y. Feng, G.T. Kokotailo, J. Am. Chem. Soc. 112 (1990) 8812.
[2] J.G. Fripiat, F. Berger-Andre, J.M. Andre, E.G. Derouane, Zeolites 3 (1983) 306.
[3] E.G. Derouane, J.G. Fripiat, Zeolites 10 (1990) 235.
[4] P.J. O'Malley, J. Dwyer, Zeolites 8 (1988) 317.
[5] R. Vetrivel, Zeolites 12 (1992) 424.
[6] R. Vetrivel, S. Pal, S. Krishnan, J. Mol. Catal. 66 (1991) 385.
[7] R. Vetrivel, C.R.A. Catlow, E.A. Colbourn, M. Leslie, Studies Surface Science and Catalysis 46 (1989) 401.
[8] A.E. Alvarado Swaisgood, M.K. Barr, P.J. Hay, A. Redondo, J. Phys. Chem. 95 (1991) 10031.
[9] K.P. Schorder, J. Sauer, M. Leslie, C.R.A. Catlow, Zeolites 12 (1992) 20.
[10] M.E. Leonowicz, J.A. Lawton, S.L. Lawton, M.K. Rubin, Science 246 (1994) 1910.
[11] G.J. Kennedy, S.L. Lawton, M.K. Rubin, J. Am. Chem. Soc. 116 (1994) 11000.
[12] J.M. Thomas, J. Klinowski, S. Ramdas, B.K. Hunter, D.T.B. Tennakoon, Chem. Phys. Lett. 102 (1982) 158.
[13] J.V. Smith, C.S. Blackwell, Nature 303 (1983) 223.
[14] S. Ramdas, J. Klinowski, Nature 308 (1984) 521.
[15] G. Engelhardt, R. Radeglia, Chem. Phys. Lett. 108 (1984) 271.
[16] R. Radeglia, G. Engelhardt, Chem. Phys. Lett. 114 (1985) 28.
[17] J.M. Newsam, J. Phys. Chem. 91 (1987) 1259.
[18] G. Engelhardt, D. Michel, High-Resolution Solid State NMR of Silicates and Zeolites, Wiley (1987), p. 129.

[19] M.J.S. Dewar, G.E. Zoebisch, F.E. Healy, J.J.P. Stewart, J. Am. Chem. Soc. 107 (1985) 3902.
[20] H. van Koningsveld, J.C. Jansen, H. van Bekkum, Zeolites 10 (1990) 235.
[21] C. Sivadinarayana, V.R. Choudhary, S. Ganapathy, J. Catal. 147 (1994) 364.
[22] C. Sivadinarayana, V.R. Choudhary, S. Ganapathy, Proc. Indian Acad. Sci. 106 (1994) 1557.
[23] J.J.P. Stewart, J. Comp. Chem. 10 (1989) 221.
[24] M. Karplus, J.A. Pople, J. Chem. Phys. 38 (1963) 2803.